



MEASUREMENT AND ENHANCEMENT OF GRAVITY DATA FOR GEOPHYSICAL INVESTIGATIONS IN ABUJA, NIGERIA

Olumba, E. and *Abubakar, T.

Department of Surveying and Geoinformatics Modibbo Adama University, Yola

*Corresponding authors' email: takana.abubakar@gmail.com

ABSTRACT

The availability of gravity data is useful to individuals, governments and organizations that wish to carry out a geophysical investigation in Abuja. The data provides an accurate model for environmental monitoring and disaster studies. This research was aimed at measurement and prediction of gravity data in Abuja, Nigeria. The aim was achieved by observation of terrestrial gravity data at forty (40) gravity stations around the federal capital territory Abuja, prediction of the gravity data at other points and the evaluation of the predicted data. Gravity reduction was carried out on the measured data to account for drift correction, free air correction, bouguer correction latitude correction and terrain correction. The data was further enhanced by interpolation using the Kriging method. A total of 59 points were predicted from the 40 measured stations. The predicted gravity anomalies were validated by comparing with their corresponding gravity anomalies obtained from the Earth Gravity Model 2008 (EGM08) because of their well-established reliability. For the number of observations, $n = 59$, the RMSE and SE were computed as 4.797mGal ($4.787 \times 10^{-5} \text{ ms}^{-2}$) and 4.880mGal ($4.880 \times 10^{-5} \text{ ms}^{-2}$) respectively. Also, the correlation value obtained was 0.991 which is significant at 0.01 level. This shows a strong relationship signifying a perfect possible agreement in the values obtained. It was therefore concluded that Kriging is a good interpolator that provides an estimate with high reliability and dependency. In this regard, considering the high cost of geophysical data collection, gravity prediction can make geophysical data collection more efficient and cost-effective.

Keywords: Gravity anomalies, Prediction, Kriging, Interpolation, Gravity model

INTRODUCTION

Geophysical surveying is a branch of applied geophysics concerned with the investigation of the subsurface of the earth. The method essentially involves taking measurements on or near the earth's surface that are influenced by the distribution of the earth's underground masses. Analysis of these measurements can reveal the physical properties of the masses including density distribution and location both vertically and laterally (Chiedu and Godwin, 1989). The method can then be applied to a range of investigations from the study of the size, shape, structure, and dynamics of the earth to the exploration of the mineral deposits and other subsurface features of the earth such as faults and anticlines. Geophysical surveying is a young science relative to other sciences discovered around 1925 (Kearey and Brooks, 1988). The geophysical surveying method is broadly classified into artificial-sourced method and natural-sourced method. The artificial-source method involves the propagation of artificial waves (e.g., seismic waves) through the earth's interior to search for local perturbation in the artificial field that may be caused by the concealed geological features while the natural-source methods are those making use of gravity and magnetic fields of the earth to search for local perturbation, in the natural fields, caused by the concealed geological features. The natural source method is logistically simpler to carry out than the artificial source method (Kearey and Brooks, 1988). Gravity Surveying is a naturally sourced method. It is a non-destructive geophysical technique that measures the difference in the earth's gravitational field at a specific location. It could be a ground gravity survey or an airborne gravity survey. The gravity method has been widely used in different applications involving engineering exploration, and regional and extensive study of geological structures where measurements of different earth gravitational fields are used to map subsurface variation in density (Biswas and Sharma, 2016; Mandal *et al.*, 2015).

Modern gravity surveying began during the first third of the twentieth century. It was said to be responsible for probably the first oil and gas exploration and continues to this day as a small but important element in the current exploration. A steady progression in instrumentation has enabled the acquisition of gravity data in nearly all environments from inside boreholes and mine shafts in the shallow earth's crust, to the undulating land surface, the sea bottom and surface, in the air, and even to the moon and other planets in our solar system. This has required a similar progression in improved methods for correcting unwanted effects and the parallel introduction of increased precision in positioning data acquisition. Significant progress in the instrumentation of gravity survey data acquisition has made gravity interpreters take advantage of this development because of the availability of computers and software today (Nabighian *et al.*, 2005). The fundamentals of the interpretation of gravity data are the same today as they were 25 years ago, but the advent of GPS and the era of small, powerful computers have revolutionized the speed and utility of the gravity method. Over the past decades, software has evolved from running on mainframes. With the availability of software running on laptop computers, data are acquired automatically and even processed and interpreted routinely in the field during data acquisition.

Gravity survey method is relatively cheap, it is also passive, that is, no energy needs to be put into the ground to acquire data; thus, the method is well suited to a populated setting. The small portable instrument used also permits walking traverses. The gravity method today is widely used in geothermal energy investigations as well as the monitoring of geothermal reservoirs under exploitation. This is because it is fairly cheap, and fast in data collection with minimum logistics preparation. The method can deduce the location of faults and permeable areas for hydrothermal movement. It is,

however, more commonly used in determining the location and geometry of heat sources.

Considerable improvements in the measurement of the earth's gravity field from the Gravity Field and Ocean Circulation Explorer (GOCE) satellite mission have provided global gravity field models with homogeneous coverage, high precision, and good spatial resolution used to detect earthquake-induced gravity changes, with the advantage of presenting homogeneous data coverage and increasing precision between different missions (Alvarez *et al.*, 2015). Ground-based gravimeters are also used to precisely measure variations in the gravity field known as the gravity anomalies at different points. Gravity anomalies are computed by subtracting a regional field from the measured field. This results in gravitational anomalies that correlate with the source body density variation. Positive gravity anomalies are associated with shallow high-density bodies whereas gravity lows are associated with shallow low-density bodies (Chiedu and Godwin, 1989).

Application of gravity to mineral deposits in environmental consideration includes lithology, structures, and at times ore bodies themselves. However, in some countries such as

Nigeria, only the seismic method is been used while the use of the gravity method is rarely noticed because of challenges in the availability of gravity data in most of the country. This has necessitated the plan of the Federal Government of Nigeria to set up the Nigeria Gravity Network Project Committee (NGNPC) to establish various gravity networks of points in Nigeria for geodetic and geophysical studies. Unfortunately, due to inexplicable reasons, the aims of this committee have not been achieved to date (Osazuwa, 1995). Gravity values and hence gravity anomalies remain inadequate for geophysical studies in Nigeria. Acquisition of gravity values for adequate gravity anomalies can be achieved by direct observation and/or mathematical estimation (Idowu, 2006). Estimation by prediction of gravity data is important to enhance the availability of the data since measurement cannot be possible everywhere (Eteje *et al.*, 2019; Nnaji *et al.*, 2021). Similarly, in this research, the study focuses on the measurement of gravity data at some point and utilizes the data to estimate other points using appropriate estimation models to enhance the availability of the data for geophysical studies in Abuja, Nigeria.

The Study Area

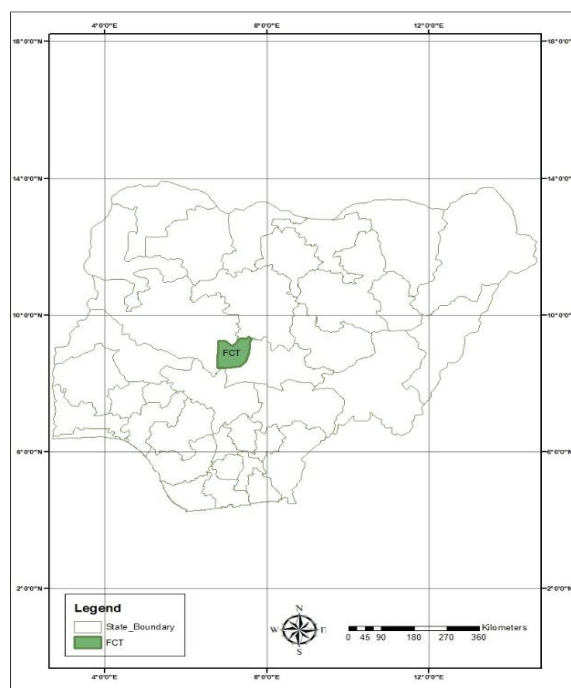


Figure 1: Map of Nigeria Showing the Study Area
Source: AGIS

Location and Size

The study area is the Federal Capital Territory Abuja. Abuja is located north of the confluence of the Niger and Benue Rivers. It is bordered by the states of Niger to the west and northwest, Kaduna to the northeast, Nasarawa to the east and south, and Kogi to the southwest. Abuja, the federal capital and a planned modern city, has a landmass of approximately 7,315 km² lying between latitudes 8.25⁰ and 9.20⁰ north of the equator and longitudes 6.45⁰ and 7.39⁰ east of Greenwich Meridian, The Federal Capital Territory is geographically located at the center of the country.

Climate

The dry seasons record the highest temperature when there are few clouds in the FCT. The location of FCT in the middle

belt region of Nigeria rids it of the extreme characteristics of climates of the North and Southern Nigeria. The region experiences two major seasons wet and dry season. Changes in temperature of as much as 17⁰C have been recorded between the highest and lowest temperature in a single say. During the rainy season, the maximum temperature is lower due to dense cloud cover. The diurnal annual range is also much lower sometimes not more than 7⁰C in July and August when its temperature ranges from 30.4⁰C and 35.1⁰C. During the dry season, relative humidity falls in the afternoon (Abuja Master Plan, 2000).

The undulating nature of the terrain also affects the temperature patterns in the FCT. The rainy season usually begins in March and ends in the middle of October in the North and early November in the South. Mean annual rainfall

ranges between 3145mm to 1631.7mm (Abuja Master Plan, 2000). As a result of its location on the windward side of the Jos Plateau, FCT experiences frequent rainfall and a noticeable increase in the mean annual total from the South to the North. The beginning and the end of the season are characterized by frequent occurrences of wind storms accompanied by thunderstorms and lightning followed by strong wind and rainfall of high intensity, but may last for just 30 minutes and then be replaced by drizzles for hours. This condition is then replaced by a few days of bright clear skies (Abuja Master Plan, 2000).

Vegetation

The vegetation of the FCT is predominantly a savannah environment. It is found between the rainforest and the poor savanna in a desert environment. An important characteristic of the savanna is the alternation of a very wet season and a very dry season, which makes plants shed their leaves in the dry season. Adakayi (2000) distinguishes the vegetation into forest and savanna. The forest consists of predominantly woody plants and without grasses, while the savanna is a vegetation type dominated by perennial mesophytic grasses with flat basal and cauline leaves. Forests are rainforest and riparian vegetation complexes. The savannah vegetation is made up of savannah woodland, park savannah, and shrub savannah. The rainforest vegetation is found in many places except the Iku and Izom plains. It is most commonly found around Gwagwa plains, river valleys, Abuchi forest reserve, foot of rocky hill, etc. The forest is evergreen with some elements of deciduous trees, which shed and regrow their leaves within two weeks. Common species here are *Antiaris Africana*, *Anthocleisa noblis*, *Ceiba pentandra*, etc. The riparian vegetation complex can be found in the valleys of river Iku, Usuma, Wuye and middle Gurara. They have a mixture of riparian woodlands, gallery forests and dense thickets. Common species are *Elaeis guineensis*, *Anogeissus leicarpus*, *Azelia Africana*

Geology and Soils

Abuja has two major geological belts, which in turn influence the local soil. These are the Precambrian basement complex and sedimentary rocks. The basement complex has a variety of rocks that can be classified into three:

- i. Rocks are made up of granites and granitic gneiss.
- ii. Rocks that consist of quartz and feldspathic quartz schists (which weathers to produce stony soils).
- iii. Rocks comprising basic igneous and metamorphic rocks such as diorite, hornblende schist, biotite schist and gneiss. These underlie low-relief regions.

The sedimentary formations also known as Nupe sandstones consist mostly of fine-grained sandstones, but with the intrusion of grits and siltstone.

We also have alluvial deposits, found around the Gurara flood plain where the river flows through the Nupe sandstone. These rock formations influence the nature of the soils. Apart from diorite and schists, the rest of the rock types give rise to sandy soils, which generally facilitate good drainage.

Based on the underlying geology, some soils have been identified in the FCT. These are:

Alluvial soils: These are found in valleys of the main rivers and streams of the FCT. The soils are narrow in coverage within the basement complex but wider within the Nupe sandstone region. These soils are moist and poorly drained almost all year round. The colour changes due to poor drainage and higher organic matter content of the surface layer.

Luvisols: These are soils washed from hilly terrains to the foot of hills as foot-plains. Local soils known as luvisols develop on these foot plains. The character of these soils varies between upper, middle and lower slopes. The lower slope bordering the alluvial valley bottom has a thick cover of sand wash material that thins at the break of the slope. The texture is loamy sand topsoil and sand clay B horizon. The middle slope is better drained, with a thin surface layer with loamy sand texture. The structure of the soil is stronger and more resistant to erosion. The soil of the upper slope occupies the highest point of the landscape. As a result, they are freely and severely drained and the depth is shallower than the middle slope. These soils are reddish brown in the top layer and reddish in the subsoil layer of the summit.

Entisols: These soils are products of inselbergs and wooded hills. They are not extensive, but they are very rocky and stony. Thus, they are referred to as skeletal soils. The soil develops near the foot of wooded hills, characterized by an abundance of rock fragments, stone and boulders in the profiles. The depth of the soil is less than 100cm and dark in colour (Balogun, 2001).

Population and Human Activities

The population of Abuja has been increasing, by natural increase and by migration with the latter exerting more influence as people migrate into the city daily. Although there are no comprehensive data to support the claim of population increase, there is enough evidence which point to the high growth of the population: the shortage of housing, employment, amenities and other facilities (Mundi, 2000). Today, almost every part of FCT has been experiencing population growth due to increased migration into the territory. However, areas with available social amenities and that offer opportunities for social, economic and political development seem to attract higher populations into them. Such areas include Garki, Wuse, Asokoro, Maitama, Bwari, Nyanya, Lugbe, Gwagwalada, Kuje, Kwali and other areas. But frankly speaking, almost all places in the FCT have a share of the population increase. The population of the city is dominated by a productive population of age i.e. below 60 years, high dependency ratio and is dominated by the male sex, as characterised by the Nigerian population. The dominance of the male sex in the FCT population can partly be explained by the fact that migration into the city by the active population in search of greener pastures is a strong factor, and men are generally more mobile than women. The structure of the population implies that FCT authorities would make extra efforts to provide consumer rather than capital goods such as housing, medical facilities, education and food. The National Population and Housing Census (2006) gave the population figures of FCT as 776, 298 people. This figure seems to be an understatement of the population of the city based on what one observes. Or one better say that since the last census, there has been a significant increase in the population of the territory.

In terms of occupational structures, the indigenes are mainly subsistence farmers. The major crops cultivated are yams, cassava, maize, guinea corn, beans, beniseed, groundnuts, melon, millet, cocoyam, etc. Apart from farming, wood and craft work is also carried out by the indigenes, especially the Gbagyis, who are also good at pottery. Wood products include mortars, pestles, tobacco pipes, masks, musical instruments, and other household utensils. The Bassa people carry out fishing activities along River Usuma, Jabi and Gurara. Ironworks are carried out by the Ganagana such as knives, hoes, dane guns, arrows and ornaments. Women do some cloth weaving (Transparency for Nigeria, 2011). Now

with the presence of migrants, who outnumber the indigenes, almost all occupations are represented in the FCT: primary, secondary and tertiary occupations.

MATERIALS AND METHODS

Materials Used

The following hardware and software were used in this research:

- i. SCINTREX CG-5 Autograv for taking gravity readings at each gravity station
- ii. High target V30 DGPS Receiver for observing X, Y, and Z coordinates of the gravity stations
- iii. ArcGIS 10.3
- iv. RASTERC™
- v. IBM SPSS Statistics 25

Methods

The methodology adopted in this research is divided into: station selection, data acquisition, data processing, and prediction.

Station Selection

The choice of station for this study started with the preliminary field inspection of the study area to locate the gravity base station. Other stations were selected and marked for the survey. A total of 40 points were used in the study. The points consisted: of a reference station at Kwali Area Council whose absolute gravity value was known and 39 new points which were chosen across the six area councils in FCT. These area councils are; Abuja Municipal, Bwari Area Council, Kuje Area Council, Gwagwalada Area Council, Kwali Area Council and Abaji Area Council.

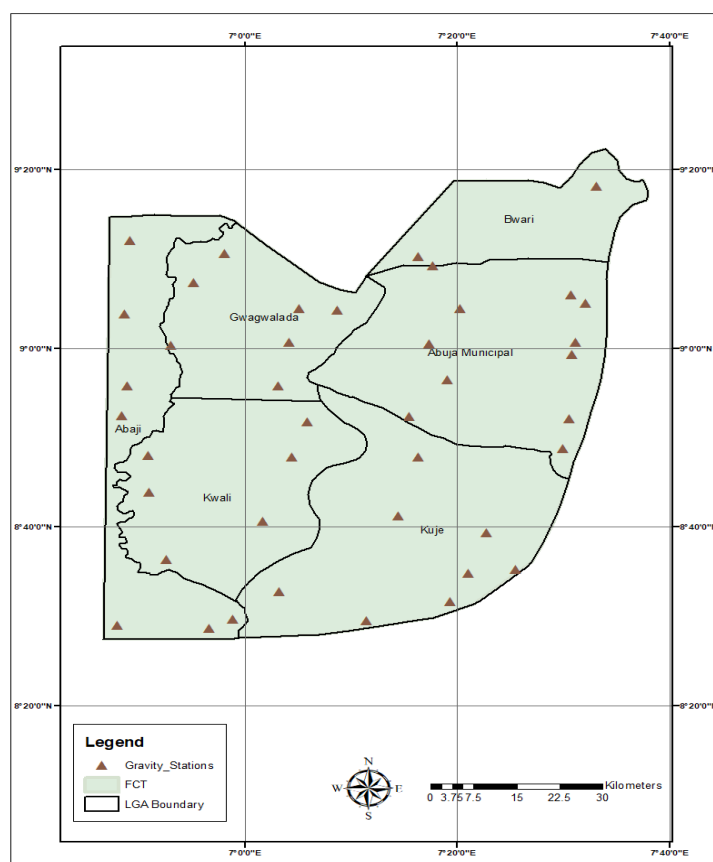


Figure 2: Selected/Observed Point Network

Data Acquisition

The data acquisition stage consisted of the GNSS and the gravity observations.

GNSS Observation

The GNSS observation was carried out using Hi-Target V30 Differential GPS in RTK mode to obtain the coordinates of the selected points. In addition to obtaining a gravity reading, a horizontal position and the elevation of the gravity station were obtained. The horizontal position was the latitude and longitude of the gravity stations.

Gravity Survey

Before setting out for the gravity survey, the instrument was first of all checked to see the calibration status. The instrument was discovered to have been calibrated for the task at hand just two days before the commencement of the survey. 40 gravity stations were selected unevenly spaced across FCT. These gravity stations served as the basis for the

prediction of further gravity points within the study area. The Survey was conducted by taking gravity readings at intervals along a traverse within the study area with SCINTREX CG-5 Autograv. To ensure the quality and consistency of the data, the expected drift of the instrument is taken into account. This was achieved by reoccupying one station (a local base station) at least every 5 hours or so. These repeated readings are performed because even the most stable gravity meter will have their readings drift with time due to elastic creep within the meter's springs and also to help remove the gravitational effects of the earth's tides readings have to be taken at a base station. The instrument drift is usually linear and less than 0.01 mGal/hour under normal operating conditions.

Data Processing

The gravity readings as well as the X, Y, and Z locations of the gravity stations observed in RTK mode were extracted

and recorded on Microsoft Excel. The observed gravity on the physical surface was subjected to corrections to reduce the observed gravity to a reference datum.

Gravity Data Reduction

The value of gravity 'g' measured on the physical surface of the earth must be different from normal gravity γ referring to the surface of the ellipsoid. A reduction of gravity value g is required to refer to g to mean sea level. Due to the effect of masses below and above the sea level, the following reductions were applied to the gravity data:

Drift Correction (D)

Correction for instrumental drift is based on repeated readings at a base station at recorded times throughout the day. The meter reading is plotted against time and drift is assumed to be linear between consecutive base readings. The drift correction was subtracted from the observed gravity value.

Free-Air correction (FAC)

The free-air correction accounts for gravity variations caused by elevation differences in the observation locations. Gravity value decreases with height, this is due to an increase in distance between the observation station and the centre of mass of the earth. FAC was applied to correct the decrease in gravity with height in free air. To reduce the observation station to datum, the following correction was applied: $FAC = 0.3086 \times H$

'H' is height in meters.

Bouguer Correction (BC)

The Bouguer correction was determined by the following equation:

$$BC = 2\pi G\rho H$$

$$2\pi G = 0.4191 \text{ (Constant)}$$

ρ is the average density of the rocks underlying the survey area in Mg/m^3 .

Latitude Correction (LC)

Correction for a given latitude is linear over about 1 km and is given by:

$$LC = 0.000812\sin(2\theta)\text{mgal/m}$$

Where θ = latitude of the observation station.

Terrain/Topographic Correction (TC)

The terrain correction is positive regardless of whether the local topography consists of a mountain or a valley (Mathews and McLean, 2015). The TC was computed using the digital elevation model derived from SRTM in SNAP4.3.2

Normal gravity (g_θ)

The international gravity formula is used to find the (g_θ) for any station located at the earth's surface using the below formula found in Al-Khafaji, and Al-Dabagh, (2019).

$$g_\theta = g_0 (1 + a\sin^2\theta - b\sin^2(2\theta))$$

where: g_0 is the gravity at the equator

a and b are constants which depend on the tilting of the earth's rotation axis. These values are 0.000053024 and -0.0000058 respectively.

θ : is the latitude angle value in degrees.

Gravity Anomaly

The gravity anomaly (Δg), is the difference between the observed gravity value (g) reduced to the geoid and a normal or theoretical, computed gravity value (g_0) at the mean earth ellipsoid, where the actual gravity potential at the geoid equals the normal gravity potential at the ellipsoid, at the projection of the same terrain point on the geoid and the ellipsoid respectively. (Dawod, 1998).

$$\Delta g = g - g_0$$

Free Air Gravity Anomaly:

Free air gravity anomaly is obtained by applying the free air correction to the difference between the observed gravity

reduced to the geoid and the theoretical gravity computed on a specific ellipsoid. The model for the computation of the free air anomaly used is the one given by Murray and Tracey (2002):

$$\Delta g_{FA} = (g_{obs} - g_0 + 0.3086H)\text{mGal}$$

Where,

Δg_{FA} = Free air anomaly

g_{obs} = Observed gravity

g_0 = Theoretical/normal gravity

H = Orthometric height

Bouguer Gravity Anomaly

The Bouguer anomaly is the difference between the observed gravity value (g_{obs}), adjusted by the algebraic sum of all the necessary corrections ($\sum corr$) and the theoretical gravity computed on a specific ellipsoid. (Raynolds, 2011).

$$\Delta g_{BA} = (g_{obs} + (\sum corr) - g_0)\text{mGal}$$

With

$$(\sum Corr) = LC + (FAC - BC) + TC$$

Where,

Δg_{BA} = Bouguer anomaly

g_{obs} = Observed gravity

g_0 = Theoretical/normal gravity

LC = Latitude correction

FAC = Free air correction

BC = Bouguer correction

TC = terrain correction

Enhancing the Gravity Data

To ensure the availability of the gravity data for effective geophysical studies, the data was predicted at grid points using the Kriging method of interpolation. Kriging method is more accurate whenever the unobserved value is closer to the observed values (Van-Beers and Kleijnen, 2003; Jassim and Altaany, 2013). The effectiveness of Kriging depends on the correct specification of several parameters that describe the semi-variogram model (spherical, exponential, gaussian), the model parameters (nugget, sill, range), drift (i.e., does the mean value change over distance) and the number of neighborhoods. Because Kriging is a robust interpolator, even a naive selection of parameters will provide an estimate comparable to many other grid estimation procedures. According to Ozturk and Kilic (2016), the basic equation used in the Ordinary Kriging is:

$$\hat{R}(x_0) = \sum_{k=0}^n w_k(x_0)R(x_k) \quad (1)$$

$R_i = R(x_i)$ are the observed values

with weights:

$$w_k(x_0),$$

$i = 1, \dots, n$ chosen such that the variance (also called kriging variance or kriging error)

$$\sigma_k^2(x_0) = \text{Var}(\hat{R}(x_0) - R(x)) = \quad (2)$$

$$\sum_{i=1}^n \sum_{j=1}^n w_i(x_0)w_j(x_0)c(x_i x_j) + \text{Var}(R(x)) - 2 \sum_{i=1}^n w_i(x_0)c(x_i x_0) \quad (2)$$

$$\text{Var}\hat{R}(x_0) = \text{Var}(\sum_{i=1}^n w_i R(x_i)) =$$

$$\sum_{i=1}^n \sum_{j=1}^n w_i w_j c(x_i x_j) \quad (3)$$

It was based on this that values of the gravity anomalies were predicted at the grid point.

Validation of the interpolated gravity data

To validate the interpolated gravity, the Earth Gravity Model (EGM2008) was used. The EGM2008 model was chosen because of its well-established reliability. The EGM2008 has a high-resolution geopotential model of the Earth's gravitational field (Wei et. al., 2020). Gravity anomalies derived from the EGM08 model were compared with their corresponding computed gravity anomalies from the

processed gravity observations to obtain the gravity anomaly residuals. The gravity anomaly residuals and the total number of selected points were used to compute the RMSE. The Root Mean Square Error, RMSE was computed using the formula given by Yilmaz and Kozlu (2018);

$$RMSE = \sqrt{\frac{1}{n} \sum_{i=1}^n (\delta\Delta g_{Res})^2} \tag{4}$$

The standard error is another measure of accuracy/reliability and it is computed using the;

$$SE = \sqrt{\frac{1}{n-1} \sum_{i=1}^n (\delta\Delta g_{Res})^2} \tag{5}$$

Where,

$$\delta\Delta g_{Res} = \Delta g_{Com} - \Delta g_{EGM}$$

Δg_{Com} = Computed gravity anomaly

Δg_{EGM08} = Model gravity anomaly (EGM08)

n = Number of Points

RESULTS AND DISCUSSION

The results of the findings in this research are presented in figures and tables. Discussions on the results obtained are similarly presented.

Table 1: Observed Bouguer anomaly data of study area

S/N	Stn_ID	LonGPS	LatGPS	ElevGPS	B. Anom	Location
1	LKJ/ABJ/079	6.94480	8.47674	134.330	127.157	Abaji Post Office
2	ABJ/YAB/001	6.78344	8.48308	132.097	123.181	YABA
3	ABJ/RUB/002	7.19312	8.47500	283.679	127.886	RUBOCHI
4	ABJ/AHI/003	7.33683	8.50679	226.807	137.492	AHINZA
5	ABJ/AHI/004	7.42660	8.58737	406.716	128.951	AHINZA 2
6	ABJ/AHI/005	7.35254	8.58020	568.642	106.644	AHINZA 3
7	ABJ/GWA/006	7.05477	8.54585	296.935	130.271	GWARGWADA
8	ABJ/DAN/007	6.87836	8.60578	201.735	115.643	DANGARA
9	ABJ/TUT/008	6.85123	8.73132	179.920	99.096	TUTU
10	ABJ/KWA/009	7.02883	8.67675	340.846	113.395	KWAITA
11	ABJ/KWA/010	7.24208	8.68674	322.287	117.158	KWAKU
12	ABJ/YAN/011	7.07565	8.79663	345.090	115.372	YANGOJI
13	ABJ/KAS/012	7.38021	8.65537	753.862	92.624	KASADA
14	ABJ/GOM/013	6.84931	8.79982	228.000	80.373	GOMANI
15	ABJ/KWG/014	6.80802	8.87382	144.916	82.977	KWAGA
16	ABJ/KIL/015	7.09980	8.86279	215.701	122.119	KILANKWA
17	ABJ/GWG/016	7.05382	8.92908	179.970	105.921	GWAGWALADA
18	ABJ/KUC/017	7.25855	8.87262	330.998	104.016	KUCHIYAKO
19	ABJ/KWA/018	6.81639	8.92955	168.712	88.056	KWAGA
20	ABJ/DOB/019	6.88544	9.00566	144.230	98.400	DOBI SOUTH
21	ABJ/PAI/020	7.07087	9.01150	191.235	104.305	PAIKO
22	ABJ/ZUB/021	7.08592	9.07397	265.067	95.109	ZUBA
23	ABJ/DOG/022	6.81246	9.06461	234.285	111.761	DOGA
24	ABJ/YEL/023	6.92112	9.12211	205.374	115.275	YELWA
25	ABJ/IBW/024	7.13180	9.14509	227.700	102.338	IBWA
26	ABJ/JIK/025	7.27273	9.17041	537.772	83.274	JIKA
27	ABJ/IZO/026	6.97002	9.17722	319.171	109.057	IZOM
28	ABJ/EGG/027	6.82096	9.20110	614.213	104.791	EGGA
29	ABJ/GOU/028	7.28996	9.00869	343.933	91.815	GOUSA
30	ABJ/LUG/029	7.31921	8.94114	362.667	94.544	LUGBE CENTRAL
31	ABJ/GUZ/030	7.52055	9.01161	635.644	73.488	GUZAPE
32	ABJ/GUR/031	7.53588	9.08363	940.960	50.597	GURKU
33	ABJ/MPA/032	7.51361	9.10036	551.309	94.961	MPAPE
34	ABJ/KAU/033	7.60282	9.31493	776.104	84.181	KAU
35	ABJ/IDU/034	7.33970	9.07394	383.124	89.855	IDU
36	ABJ/JIB/035	7.29677	9.15385	726.465	62.026	JIBI
37	ABJ/WAS/036	7.51046	8.86868	596.447	86.413	WASA
38	ABJ/KPA/037	7.51426	8.98763	640.106	72.986	KPADUMA
39	ABJ/KAR/038	7.55652	8.78489	501.823	95.108	KARSHI SOUTH
40	ABJ/PAG/039	7.27363	8.79747	410.815	111.020	PAGI

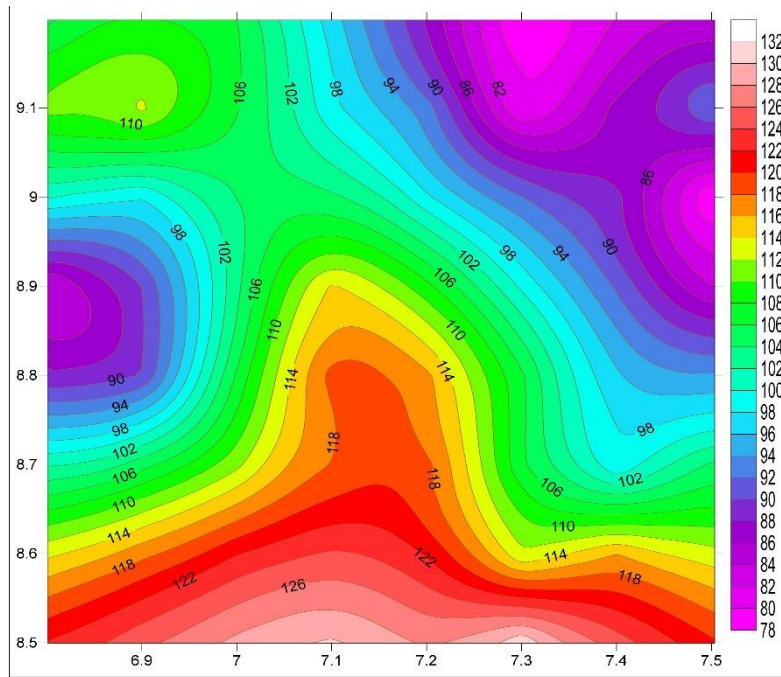


Figure 3: Contour map of Bouguer anomaly of the study area.

Table 2: Predicted Bouguer anomalies, EGM08-derived Bouguer anomalies and residual

S/N	Stn No	LON	LAT	Δg_{Com}	Δg_{EGM08}	$\delta \Delta g_{Res}$
1	P1	6.80118	9.19698	105.692	111.03560	-5.344
2	P2	6.90223	9.19493	108.324	108.50372	-0.180
3	P3	7.00098	9.19612	106.024	111.27062	-5.247
4	P4	7.30052	9.19768	78.105	78.26167	-0.157
5	P5	7.40010	9.19792	82.217	82.56367	-0.347
6	P6	7.50004	9.19863	84.205	88.24167	-4.037
7	P7	6.80047	9.09847	110.492	110.39066	0.101
8	P8	6.90112	9.09776	112.301	114.96766	-2.667
9	P9	7.00034	9.09990	106.129	105.90096	0.228
10	P10	7.10099	9.09919	98.492	98.15867	0.333
11	P11	7.20164	9.09990	92.782	95.03867	-2.257
12	P12	7.30015	9.09919	80.048	79.81467	0.233
13	P13	7.40009	9.09990	86.633	86.51633	0.117
14	P14	7.50003	9.10133	92.304	92.24521	0.059
15	P15	7.50075	8.99947	78.004	81.15700	-3.153
16	P16	7.40057	9.00044	88.412	88.31556	0.096
17	P17	7.30063	8.99949	92.102	92.42107	-0.319
18	P18	7.20164	9.00139	98.091	97.75267	0.338
19	P19	7.10075	9.00139	104.221	104.12766	0.093
20	P20	7.00082	8.99949	104.084	105.46066	-1.377
21	P21	6.90183	9.00044	98.308	98.15467	0.153
22	P22	6.80094	9.00139	100.521	100.27200	0.249
23	P23	6.80094	8.90031	84.048	86.99810	-2.950
24	P24	6.90088	8.90126	90.217	89.90801	0.309
25	P25	7.00082	8.90031	103.567	103.86311	-0.296
26	P26	7.09980	8.90031	114.19	116.34942	-2.159
27	P27	7.20259	8.90031	108.327	108.44501	-0.118
28	P28	7.30158	8.90031	99.372	99.50790	-0.136
29	P29	7.40057	8.90126	91.583	91.64131	-0.058
30	P30	7.50050	8.90031	84.025	87.75268	-3.728
31	P31	7.50336	8.79847	94.346	94.41731	-0.071
32	P32	7.40057	8.79847	96.341	96.53700	-0.196
33	P33	7.30158	8.79961	106.2	109.99521	-3.795
34	P34	7.20259	8.79866	116.304	116.41860	-0.115
35	P35	7.10075	8.80057	118.753	118.93193	-0.179

36	P36	7.00177	8.79866	106.673	106.59009	0.083
37	P37	6.90183	8.79866	90.29	97.24463	-6.955
38	P38	6.80094	8.79961	88.471	88.56968	-0.099
39	P39	6.80189	8.69768	102.049	102.15797	-0.109
40	P40	6.90088	8.69768	105.574	109.93171	-4.358
41	P41	7.00177	8.69768	111.748	111.85648	-0.108
42	P42	7.10075	8.69768	118.163	117.95260	0.210
43	P43	7.20259	8.69768	118.397	123.15179	-4.755
44	P44	7.30063	8.69863	106.391	106.60421	-0.213
45	P45	7.40057	8.69863	98.417	98.53383	-0.117
46	P46	7.50146	8.69949	104.419	104.46432	-0.045
47	P47	7.39997	8.59845	116.209	116.13052	0.078
48	P48	7.29944	8.59726	112.541	112.41360	0.127
49	P49	7.20188	8.59726	121.804	127.02321	-5.219
50	P50	7.10016	8.59786	124.371	124.20157	0.169
51	P51	7.00022	8.59726	122.106	121.96511	0.141
52	P52	6.90040	8.59750	117.583	117.76290	-0.180
53	P53	6.80047	8.59845	113.618	113.44879	0.169
54	P54	6.80142	8.50137	122.039	121.81371	0.225
55	P55	6.90136	8.49947	125.494	128.31530	-2.821
56	P56	7.00034	8.49947	128.557	128.35131	0.206
57	P57	7.10028	8.49947	130.283	130.47311	-0.190
58	P58	7.20117	8.50137	127.491	127.33410	0.157
59	P59	7.30110	8.49947	131.542	135.82002	-4.278

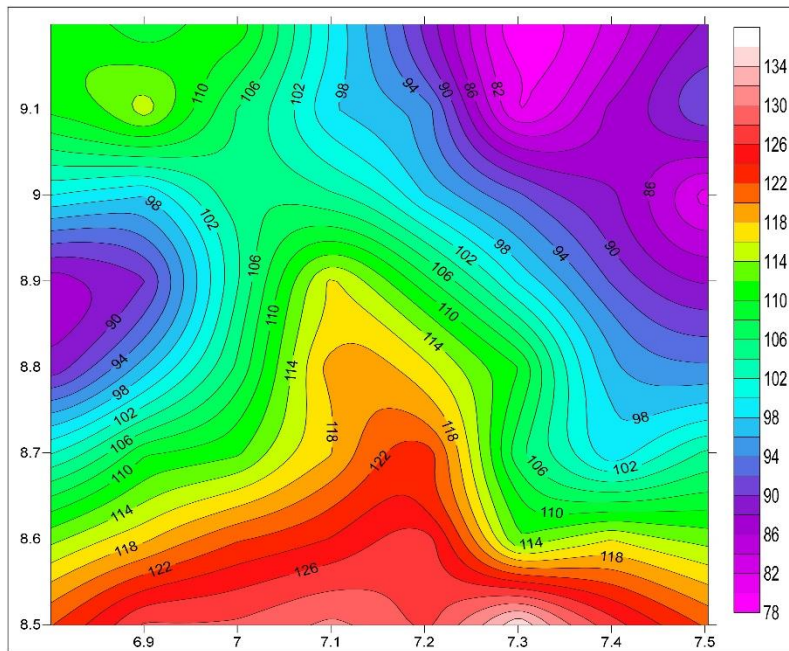


Figure 4: Contour map of predicted Bouguer anomaly

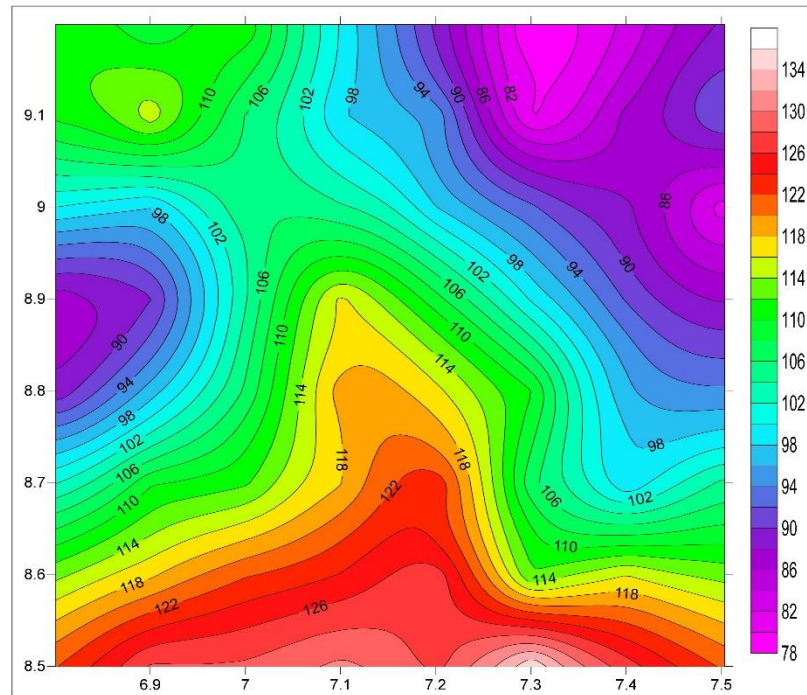


Figure 5: Contour map of EGM08 derived Bouguer anomaly

Discussion of Result

Table 1 and Figure 3, show the complete Bouguer anomaly and its contour map of the study area respectively. From the complete Bouguer anomaly map, it was shown that the Bouguer anomaly ranges from 50Mgal to 138Mgal. This is similar to the work of Balogun and Osazuwa (2023) where they did a work on the gravity field over the whole of Nigeria, 59 gravity stations were involved. They published many gravity maps including the Bouguer gravity anomaly map. Table 2 above shows the predicted Bouguer anomaly and the EGM08-derived anomaly. The predicted complete Bouguer ranges from 78Mgal to 132Mgal showing that the predicted values all lie within the study area. Similarly, Eteje *et al.*, (2019) in their study, also determined the absolute gravity values of some selected points, computed their local gravity anomalies and used an interpolation surface to enable the gravity anomaly of any points of unknown coordinates to be determined by interpolation within Benin City. Figures 4 and 5 are the contour plots of the predicted and EGM08-derived Bouguer gravity anomalies. This is similar to Balogun and Osazuwa (2023), where they determined the bouguer gravity anomaly and the map was equally published.

In Table 2, the residuals ($\delta\Delta g_{Res.}$) between the predicted and model gravity anomaly was computed. This was used to obtain the Root mean square error (RMSE) and Standard error (SE) from equations 4 and 5 respectively. For the number of observations, $n = 59$, the RMSE and SE were computed as 4.797mGal ($4.787 \times 10^{-5} \text{ ms}^{-2}$) and 4.880mGal ($4.880 \times 10^{-5} \text{ ms}^{-2}$) respectively. The result obtained shows there is high reliability, as well as dependability between the two sets of data.

Furthermore, a correlation analysis was carried out to determine the relationship between the predicted and the EGM08-derived data. The coefficient of correlation was found to be 0.991. This shows a strong relationship between the two sets of data

CONCLUSION

In this research, gravity data for forty (40) gravity stations around Abuja, Nigeria were obtained by terrestrial gravity observation. The data were reduced using suitable gravity reduction methods to a complete Bouguer gravity anomaly. 59 other points were predicted by the kriging method of interpolation and the result obtained was compared with the EGM08-derived gravity data for authentication. The two data, from the analysis show that they agree. This is evident from the computed coefficient of correlation that was found to be 0.991. This shows a strong relationship between the two sets of data

It can therefore be concluded that the data were successfully measured and enhanced using a kriging interpolator. The kriging interpolator uses a simple selection of parameters which includes semi-variogram model, nugget effect, range, drift terms, number of neighbors, weighting method and coordinate system that provide an estimate with high reliability and dependency. In this regard, considering the high cost of geophysical data collection, gravity data can be measured in a few places and enhanced with a predictor model for more efficient and cost-effective geophysical studies.

REFERENCES

- Balogun, B.B. and Osazuwa, I.B., (2023). The gravity field and gravity data reduction across the continental area of Nigeria. *Geodesy and Geodynamics* (Elsevier), 14, 304-320
- Dawod, D. M., (1998). A National Gravity Standardization Network for Egypt. Published Ph.D. dissertation of the Department of Surveying Engineering, Shoubra Faculty of Engineering, Zagazig University. http://www.academia.edu/794554/The_egyptian_national_gravity_standardization_network_ENGN97. Accessed 15th February, 2021

Ellman A., Vanicek P., Santos M. and R. Kingdon, (2007). "Interrelation between the geoid and Exploration.

- Eteje, S. O., Oduyebo O. F. and Oluyori P D. (2019). Modelling Local Gravity Anomalies from Processed Observed Gravity Measurement for Geodetic Applications. *International Journal of Scientific Research in Science and Technology (IJRST)*, Vol. 6, No. 5, PP 144-162.
- Idowu T. O. (2006). Prediction of Gravity Anomalies for Geophysical and Exploration. *FUTY Journal of the Environment, Yola-Nigeria* Vol. 1 No.1, July 2006
- Jassim, F. A. and Altaany, F. H. (2013). Image Interpolation Using Kriging Technique for Spatial Data. *Canadian Journal on Image Processing and Computer Vision*, Vol. 4, No. 2, pp 16-21.
- Kearey, P. and Brooks, M. (1988). *An Introduction to Geophysical Exploration*. The Garden City, Blackwell Scientific Press, Letchworth, Herts.
- Mandal A. Biswas A. Mittal S. Mohanti W.k., Sharma S. P., Sengupta D., Sen J., Bhatt A.K. (2013). Geophysical Anomalies Associated with Uranium Mineralization from Beldih Mine, South Perugia Shear Zone India. *J. Geol Soc.ind* 82(6):601-606
- Mathews, L. R., Mclean, M. A. (2015). Gippsland Basin Gravity Survey. Geological Survey of Victoria Technical Record. http://earthresources.vic.gov.au/data/assets/pdf_file/0011/456743/G6-Gippsland-gravity-survey-report-june-2015.pdf . Accessed 23 February 2021.
- Mundi, R., (2000). "Population of the FCT" in *Geography of the Federal Capital Territory*. Dawam, P.D. (eds). Minna. Famous Ashanlu publishers. Pp70-84.
- Murray, A. S., Tracey, R. M. (2001). Best Practice in Gravity Surveying. Australian Geological Survey Organization. <https://d28rz98at9flks.cloudfront.net/37202/37202.pdf> . Accessed 23 February, 2021.
- National Population Commission (2006). Population and Housing Census of the Federal Republic of Nigeria.
- Nnaji, O.A., Udensi, E.E., Unuevho, C., Lawrence, J.O. and Salako, K.A., (2021). Estimation of the depth to Moho of parts of North Central Nigeria using Bouguer gravity data. *Journal of Science, technology, mathematics and education, (JOSTMED)* 17, (12), 35-43.
- Nabighian, M.N., Ander, M.E., Grauch, V.J.S., Hansen, R.O., LaFehr, T.R., Li, Y.1 , Pearson, W.C., Peirce, J.W., Phillips, J.D. , and Ruder, M.E. (2005), The Historical Development of the Gravity Method in Exploration VL70 DO - 10.1190/1.2133785 Geophysics
- Osazuwa, I. B. (1995). Nigeria gravity network project: achievements and challenges. Proceedings of the second Regional Geodesy and Geophysics Assembly in Sweden.
- Ozturk, D. and Kilic, F. (2016). Geostatistical Approach for Spatial Interpolation of Meteorological Data. *Anais da Academia Brasileira de Ciências*, Vol. 88, No. 4, pp 2121-2136.
- Raynolds, J. M. (2011). "An Introduction to Applied and Environmental Geophysics. Geophysics (2nd ed). Published by John Wiley & Sons Ltd. West Sussex, England.
- Transparency for Nigeria (2011). About Nigeria, Abuja, FCT. Transparency for Nigeria. Available online at [www.http//transparencynigeria.com/index.php?option](http://transparencynigeria.com/index.php?option)
- Van-Beers, W. C. M. and Kleijnen, J. P. C. (2003). Kriging for Interpolation in Random Simulation. *Journal of the Operational Research Society*, Vol. 54, pp. 255–262. In Jassim, F. A. and Altaany, F. H. (2013). Image Interpolation Using Kriging Technique for Spatial Data. *Canadian Journal on Image Processing and Computer Vision*, Vol. 4, No. 2, pp 16-21.
- Wei Liang, Jiancheng Li, Xinyu Xu, Shengjun Zhang, Yongqi Zhao, (2020,) A High-Resolution Earth's Gravity Field Model SGG-UGM-2 from GOCE, GRACE, Satellite Altimetry, and EGM2008, Engineering, Volume 6, Issue 8, Pages 860-878,ISSN 2095-8099, <https://doi.org/10.1016/j.eng.2020.05.008>. (<https://www.sciencedirect.com/science/article/pii/S2095809919305661>)
- Yilmaz, M. and Kozlu, B. (2018). The Comparison of Gravity Anomalies Based on Recent High-Degree Global Models. *Afyon Kocatepe University Journal of Science and Engineering*, Vol. 18, pp 981-990.



©2024 This is an Open Access article distributed under the terms of the Creative Commons Attribution 4.0 International license viewed via <https://creativecommons.org/licenses/by/4.0/> which permits unrestricted use, distribution, and reproduction in any medium, provided the original work is cited appropriately.